THE JOURNAL OF PHYSICAL CHEMISTRY C LETTERS

2007, *111,* 1061−1064
Published on Web 12/23/2006

Two-Dimensional Self-Organization of CdS Ultra Thin Films by Confined Electrochemical Atomic Layer Epitaxy Growth

Massimiliano Cavallini,*,† Massimo Facchini,† Cristiano Albonetti,† Fabio Biscarini,† Massimo Innocenti,‡ Francesca Loglio,‡ Emanuele Salvietti,‡ Giovanni Pezzatini,‡ and Maria Luisa Foresti*,‡

CNR-ISMN Bologna Research Division "Nanotechnology of Multifunctional Materials", Via P. Gobetti 101, I-40129 Bologna, Italy, and Department of Chemistry, Università di Firenze, Via della Lastruccia 3, I-50019 Sesto Fiorentino (FI), Italy

Received: October 20, 2006; In Final Form: December 7, 2006

We present a method that uses patterned self-assembled monolayers (SAMs) of alkanethiolates on silver as templates to fabricate ordered two-dimensional arrays of solid CdS nanoclusters. The CdS is grown by electrochemical atomic layer epitaxy inside sub-micrometric stripes of hexadecanthiol SAM fabricated by microcontact printing. CdS ultrathin films grow and self-organize into an ordered pattern of nanoclusters. This pattern exhibits both lithographically imposed ordered structures and a self-affine structure along the direction perpendicular to the stripes. On the contrary, along the direction parallel to the stripes no spatial correlation among the clusters has ever been observed.

II-VI semiconductors are well-known materials used for many applications in science and technology. They have special relevance on sensors,[1] photovoltaic,[2] photoelectrochemical cells[3] and more generally nanoscience.[4]

Several deposition techniques have been used to grow thin films of II−VI semiconductors, among them, chemical vapor deposition,[5] molecular beam epitaxy,[6] reactions in Langmuir−Blodgett films,[7] electrochemical atomic layer epitaxy (ECALE),[8] and pulsed electrochemical deposition.[9] All of these methods are flexible and capable of generating supported planar arrays of a variety of semiconductor nanocrystallites. However, they have limited control in size distribution and spatial arrangement while the technology requires the control of these parameters.[10]

The fabrication of ordered two-dimensional arrays of II−VI semiconductor microparticles has been reported using confined precipitation[11] and direct microcontact printing of CdS nanoclusters previously synthesized.[12]

The electrochemical deposition on thiolate pre-patterned surface has been reported several times for the electrodeposition of metals, including nikel electrodeposited on gold,[13,14] gold/silver electrodeposited on gold,[15,16] and Cu electrodeposited on printed SAM.[17] Recently, Seo et al. reported nanoshaving combined with silver electrodeposition on Au(111).[18]

Here, we investigate for the first time how, by confining the growth of CdS thin films by combined ECALE, CdS nanoclusters grow and self-organizes into an ordered pattern organized at nanoscale. This pattern exhibit both lithographically imposed ordered structures and a self-affined structuration[19] along preferential directions.

ECALE technique exploits the underpotential deposition (UPD) process to synthesize material at the working electrode.[20] The method is based on the alternate electrodeposition of the elements that form the compound at underpotential (see Figure 1). The UPD is a surface-limited phenomenon whereby, the deposition of one element occurs at a potential preceding the Nerstian equilibrium value. The layer-by-layer electrodeposition on single-crystal faces allows submonolayer control of film thickness and yields semiconducting nanostructures of high crystallinity.[21]

Here, we confined the growth of CdS by ECALE inside submicrometric stripes of hexadecanthiol SAM obtained by microcontact printing (μCP).[22] The presence of SAM patterns reduces the available area for electrodeposition to 60%, since in this range of potential of the UPD it acts as insulator.[23] The confinement induces a dramatic change in morphology of CdS thin film.

In our experiments, the stamp consists of parallel lines 410 nm wide and 100 nm deep and a periodicity between lines of 740 nm. Figure 2a shows the cyclic voltammograms of UPD of sulfur on bare Ag(111) (curve 1) and on patterned Ag(111) (curve 2).

The presence of μ-stripes does not change the potential range of UPD, whereas the decrease in the cyclic voltammogram peaks indicates a reduction of the available surface for ECALE.

The effective quantity of deposited CdS was confirmed by measuring the charge involved in the stripping of Cd, followed by the stripping of S (Figure 2b). The charges involved in Cd stripping for a given number of cycles coincide with the corresponding charges of S, thus indicating the expected 1:1 stoichiometric ratio. Moreover, these charges are linear functions

* To whom correspondence should be addressed. Phone: +390516398519. Fax: +390516398539. E-mail: m.cavallini@bo.ismn.cnr.it (M.C.); foresti@unifi.it (M.L.F.).
† CNR-ISMN Bologna Research Division "Nanotechnology of Multifunctional Materials".
‡ Università di Firenze.

10.1021/jp0668908 CCC: $37.00

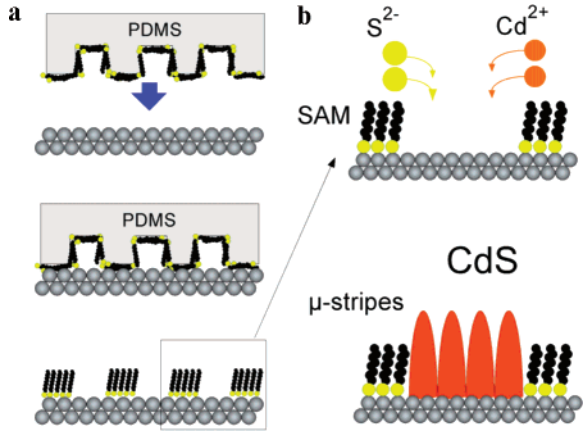

Figure 1. (a) Scheme of microcontact printing: the thiols form submicrometric stripes (μ-stripes) of SAM on Ag surface. (b) Scheme of electrochemical atomic layer epitaxy on patterned surface.

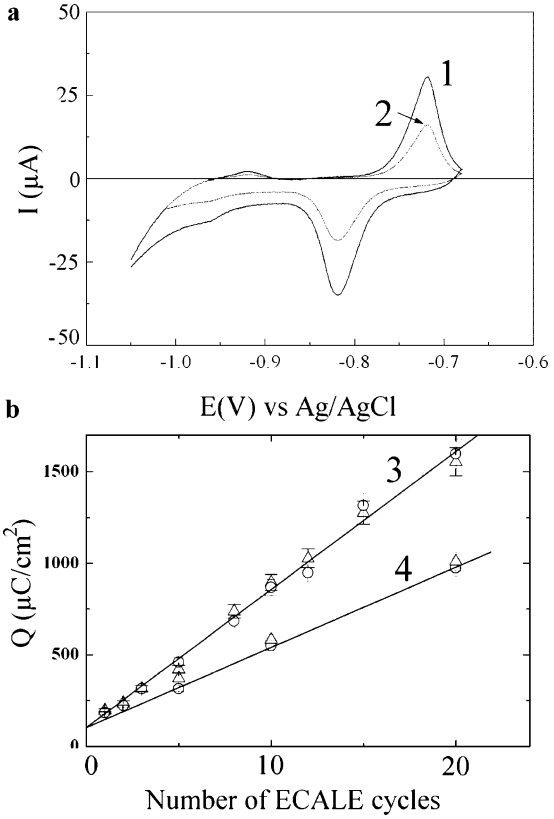

Figure 2. (a) Cyclic voltammograms for the oxidative sulfur UPD from a solution of 0.5 mM, Na_2S in pH 9.6 ammonia buffer on bare Ag(111) (curve 1) and on patterned Ag(111) (curve 2). (b) Plots of the charge involved in the oxidative stripping of cadmium (△) and the reductive stripping of sulfur (○) as a function of the number of ECALE cycles on bare Ag(111) (curve 3) and on patterned Ag(111) (curve 4).

of the number of deposition cycles, thus indicating that the same amount of the compound is deposited in each cycle and, therefore, confirming layer-by-layer growth.

Apart from the amount of the elements deposited in each cycle, this behavior coincides with that obtained on the bare Ag(111). The slope of each plot gives the charge per cycle. The slope of 43 μC cm^{-2} obtained on a patterned surface amounts to 61% of the slope, obtained on the bare surface (70 μC cm^{-2}). This is in perfect agreement with the value of the free surface of silver as detected by AFM measurements (see details in the Supporting Information).

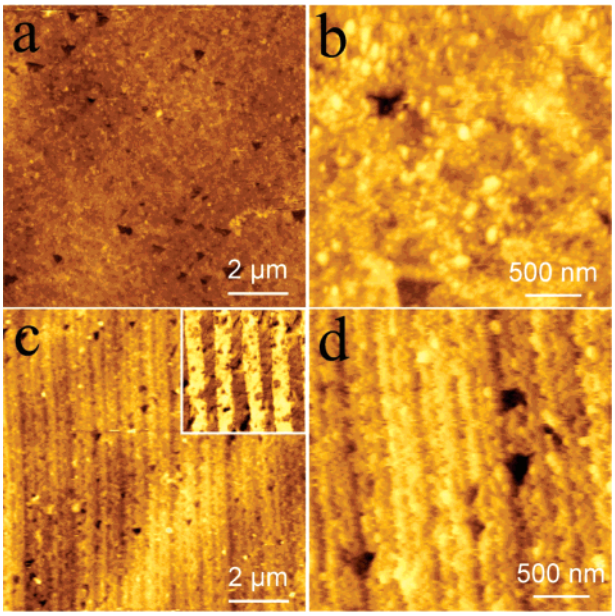

Figure 3. (a) 10 × 10 μm^2 morphology of 20 cycles (corresponding to 40 Å) of CdS thin film grown by ECALE on Ag(111). (b) Detail of a (c) 10 × 10 μm^2 morphology of 20 cycles of CdS thin film grown by ECALE on patterned Ag(111). The inset shows lateral force microscopy image of patterned surface. (d) Detail of c. between the printed μ-stripes of hexadecanethiol, the CdS clusters self-organize along parallel nanostripes.

The characterization was completed with a morphological investigation performed on samples.

Figure 3 shows AFM images of CdS thin film formed with 20 ECALE cycles, which correspond to a film thickness of about 40 Å. On a bare surface (Figure 3a,b), CdS forms nanoclusters that are randomly distributed over the whole surface; their diameter ranges from 50÷90 nm (Figure 3b) in good agreement with previously reported data on bare Ag(111).[24]

The film morphology dramatically changes on patterned surfaces (Figure 3c,d). CdS grows only in the zones free of the SAM; therefore, its growth is confined between the μ-stripes. Figures 3d shows details of CdS nanoclusters grown inside two μ-stripes of SAM. Although occasionally we observed a random distribution of nanoclusters, they were usually aligned along nanostripes with a periodicity of about 170 nm oriented like the μ-stripes (Figure 3d).

No relevant difference in morphology was observed depending on the order of whether Cd or S is deposited first.

At sub-micrometric scale, the roughness of the substrate is comparable with the roughness of the CdS thin film, and for this reason, the differences between the regions containing CdS and the regions containing the SAM are not clearly evident in the topography without the help of image analysis. In order to highlight (qualitatively) the regions where the CdS was grown, we performed lateral force microscopy (LFM), which is sensitive to the mechanical differences (local "friction") on the surface.[25] The LFM shows a contrast in between the zones where the CdS film has been grown and the zones containing the SAM (see inset of Figure 3c).

Figure 4 shows the statistical analysis of nanoclusters distribution corresponding to Figure 3d. Whereas in the CdS grown on bare Ag both the autocorrelation map and power spectral density (PSD) are isotropic, on the patterned surface, both of them exhibit an anisotropy with respect the direction of printed stripes. The 2D height−height correlation function "$g(r)$" (Figure 4a) shows the periodicity of the printed lines.

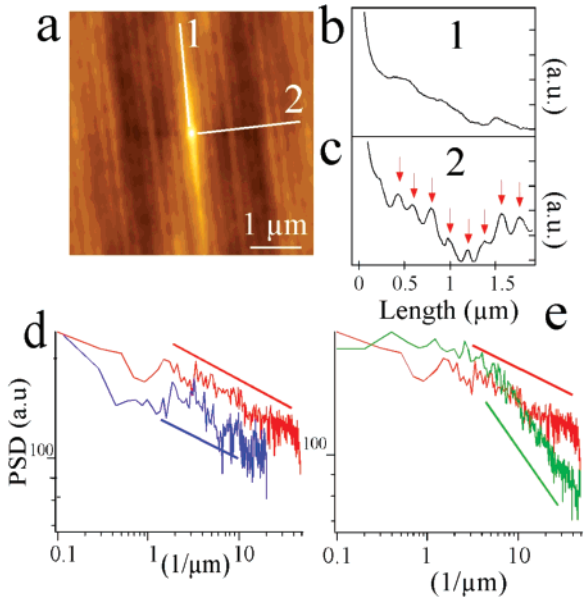

Figure 4. (a) 2D height−height correlation function $g(r)$ of CdS thin film grown on patterned surface (corresponding to Figure 3c,d). (b) Line profile of $g(r)$ measured parallel (line 1) and (c) perpendicular (line 2) to the printed μ-stripes of SAM. (d) Power spectral density measured from the AFM topographic image measured in the direction parallel to the printed μ-stripes (green curve) and AFM topographic image of CdS grown on bare Ag (red curve). The continuous lines are guide for eyes. The change in the growth exponent is evident. (e) Power spectral density measured in the direction perpendicular to the printed μ-stripes (blue curve) and AFM topographic image of CdS grown on bare Ag (red curve) as shown by the guide for eyes, the growth exponent is almost the same.

Although the $g(r)$ measured parallel to the μ-stripes (Figure 4b, line 1) does not show a spatial correlation, the $g(r)$ measured perpendicular to the μ-stripes of SAM (Figure 4b, line 2) shows an evident spatial correlation among the nanoclusters, which extends up to the eighth neighbor (the peaks in the correlation function are indicated with red arrows). The power spectral density (PSD) measured perpendicular to the printed μ-stripes (Figure 4e) confirms that the topographic fluctuations are spatially correlated; furthermore, they exhibit a self-affine structure. Self-affines are defined as structures that preserve a similar morphology upon a change of magnification and after a rescaling of the third dimension (z axis). For a self-affine surface, roughness scaling follows a power law with a growth exponent β and a scaling exponent α, which distinguish the growth universality class.[26] As in the case shown in Figure 4e, a self-affine structure exhibits a power-law decay of PSD in a finite range of spatial frequency.

Figure 4e shows the PSD measured perpendicular to the printed μ-stripes and the PSD of CdS grown on bare surface. The PSD exhibits two distinct regions, a plateau at low spatial frequencies, which indicates the absence of spatial correlations, and a region which exhibits a power-law decay at higher spatial frequencies. The steeper portion of the latter is taken as the self-affine range.

As shown in Figure 4e, the PSD of CdS growth on the patterned surface exhibits a different slope (i.e., growth exponent) in the linear region, which indicates a difference in the mechanism of growth.[26,27]

On the other hand, in the direction parallel to the μ-stripes PSD exhibits almost the same slope of CdS growth on the bare surface (Figure 4d); in this direction, although the self-affinity is not clear, it cannot be excluded. This behavior suggests that on the direction parallel to the μ-stripes the presence of μ-stripes does not influence significantly the CdS growth. A more detailed study of the mechanism of growth is under investigation, and it will be the subject of a future paper.

Summarizing, we present, for the first time, an application of the ECALE process combined with μCP that allows the fabrication, by spontaneous organization, of an ordered array of nanoclusters of CdS. We proved that the UPD phenomena, exploited by the ECALE method, works in the presence of μ-stripes without relevant effect on the electrochemistry of the process, but it has a strong influence in the film morphology. We demonstrate that the presence of stripes confines the growth of CdS ultrathin film that it self-organizes in a spatially correlated pattern of nanoclusters, which exhibit a self-affine structure.

Our approach opens new perspectives to soft-lithography combined with electrochemistry. Future developments are in progress and include the confinement growth inside a two-dimensional cell with a different shape and the progressive reduction of the size of the confinement.

Acknowledgment. This work was partly supported by ESF-SONS project FUNSMARTS, Fondo Investimenti Ricerca di Base (FIRB) NOMADE, the Consorzio Interuniversitario per la Scienza e Tecnologia (INSTM), and Monte dei Paschi di Siena (MPS). We thank Rajendra Kshirsagar for stimulating discussion and suggestions.

Supporting Information Available: Details of experiments: substrate preparation, stamps preparation, microcontact printing, and atomic force microscopy setup. This material is available free of charge via the Internet at http://pubs.acs.org.

References and Notes

(1) Guliants, E. A.; Schwarb, R.; Bearbower H.; Gord, J. R.; Bunker, C. E. *Rev. Adv. Mater. Sci.* **2005**, *10*, 289.
(2) Shah, A.; Torres, P.; Tschanner, R.; Wyrsch, N.; Keppner, H. *Science* **1999**, *285*, 692.
(3) Britt, J.; Ferekides, C. *Appl. Phys. Lett.* **1993**, *62*, 285.
(4) Chen, S.; Wang, Z. L.; Ballato, J.; Foulger, S. H.; Carroll, D. L. *J. Am. Chem. Soc* **2003**, *125*, 16187.
(5) Liu, D. C.; Lee, C. P. *Appl. Phys. Lett.* **1993**, 63, 3503.
(6) Notzel, R.; Niu, Z.; Ramsteiner, M.; Schonherr, H. P.; Tranpert, A.; Daweritz, L.; Ploog, K. H. *Nature* **1998**, *392*, 56.
(7) Zhao, X. K.; Fendler, J. H. *J. Phys. Chem.* **1991**, *95*, 3716.
(8) Gregory, B. W.; Suggs, D. W.; Stickney, J. L. *J. Electrochem. Soc.* **1991**, *138*, 1279.
(9) Kolb, D. M.; Ullmann, R.; Will, T. *Science* **1997**, *275*, 1097.
(10) Cavallini, M.; Stoliar, P.; Moulin, J. F.; Surin, M.; Leclere, P.; Lazzaroni, R.; Breiby, D. W.; Adreasen, J. W.; Nielsen, M. M.; Sonar, P.; Grimsdale, A. C. *Nano Lett.* **2005**, *5* (12), 2422.
(11) Qin, D.; Xia, Y.; Xu, B.; Yang, H.; Zhu, C.; Whitesides, G. M. *Adv. Mater*. **1999**, *11*, 1433.
(12) Santhanam, V.; Andres, R. P. *Nano Lett.* **2004**, *4*, 41.
(13) Moffat, T. P.; Yang, H. J. *Electrochem. Soc.* **1995**, *142* (11), L220.
(14) Kumar, A.; Biebuyck, H. A.; Whitesides, G. M. *Langmuir* **1994**, *10* (5), 1498.
(15) Pesika, N. S.; Fan, F. Q.; Searson, P. C.; Stebe, K. J. *J. Am. Chem. Soc.* **2005**, *127*, 11960.
(16) Pesika, N. S.; Radisic, A.; Stebe, K. J.; Searson, P. C. *Nano Lett.* **2006**, *6*, 1023.
(17) Kim, S.-K.; Kim, J. J. *Electrochem. Solid State Lett.* **2004**, *7*, C98.
(18) Seo, K.; Borguet, E. *Langmuir* **2006**, *22*, 1388.
(19) Melucci, M.; Gazzano, M.; Barbarella, G.; Cavallini, M.; Biscarini, F.; Maccagnani, P.; Ostoja, P. *J. Am. Chem. Soc.* **2003**, *125*, 10266.
(20) Foresti, M. L.; Pezzatini, G.; Cavallini, M.; Aloisi, G.; Innocenti, M.; Guidelli, R. *J. Phys. Chem. B* **1998**, *102*, 7413.
(21) Foresti, M. L.; Pozzi, A.; Innocenti, M.; Loglio, F.; Pezzatini, G.; Salvietti, E.; Giusti, A.; D'Anca, F.; Felici, R.; Borgatti, F. *Electrochim. Acta* **2006**, *51*, 5532.
(22) Wilbur, J. L.; Kumar, A.; Kim, E.; Whitesides, G. M. *Adv. Mater*. **1994**, *6*, 600.

(23) Finklea, H. O. In *Electroanalytical Chemistry*; Bard, A. J., Rubinstein, I., Eds.; Marcel Dekker: New York 1996; Vol. 19, pp 109−335.
(24) Innocenti, M.; Cattarin, S.; Cavallini, M.; Loglio, F.; Foresti, M. L. *J. Electroanal. Chem.* **2002**, *532*, 219.
(25) Meyer, E., Lüthi, R.; Howald, L.; Gutmannsbauer, W.; Haefke H.; Güntherdot, H.-J. *Nanotechnology* **1996**, *7*, 340.
(26) Barabási, A.-L.; Stanley, H. E. *Fractal Concepts in Surface Growth*; Cambridge University Press: Cambridge, U.K., 1995.
(27) Schwarzacher, W. *J. Phys.: Condens Matter*. **2004**, *16*, R859.